Dark states with electromagnetic form factors at electron colliders

Yu Zhang,[1] Mao Song,[2] and Liangwen Chen[3,4,*]

[1]*School of Physics, Hefei University of Technology, Hefei 230601, China*
[2]*School of Physics and Optoelectronics Engineering, Anhui University, Hefei 230601, China*
[3]*Institute of Modern Physics, CAS, Lanzhou 730000, China*
[4]*Advanced Energy Science and Technology Guangdong Laboratory, Huizhou 516000, China*

(Received 8 October 2022; accepted 22 February 2023; published 15 March 2023)

Electromagnetically neutral dark sector particles may feebly interact with photons through higher dimensional effective operators, such as mass-dimension-five magnetic and electric dipole moment, and a mass- dimension-six anapole moment and charge radius operators. In this work, we use hypercharge gauge field form factors to treat dark states, which will induce not only electromagnetic form factors but also the corresponding Z boson operators. Taking a Dirac fermion χ as an example, we investigate the probes of searching for such dark states at current and future e^+e^- collider experiments including BESIII, STCF, Belle II, and CEPC via monophoton searches. Compared with current experiments, we find that electron colliders including BESIII, STCF, and Belle II, which operate with the center of mass at several GeV, have leading sensitivity on the corresponding electromagnetic form factors for the mass-dimension-five operators with dark states lighter than several GeV, while they cannot provide competitive upper limits for the mass-dimension-six operators. Future CEPC operated with the center of mass on and beyond the mass of Z boson with competitive luminosity can probe the unexplored parameter space for dark states with mass-dimension-five (six) operators in the mass region of $m \lesssim 100$ GeV (10 MeV $\lesssim m \lesssim 100$ GeV).

DOI: 10.1103/PhysRevD.107.055023

I. INTRODUCTION

The primary importance for our understanding of elementary interactions is shedding light on the dark-sector states. Searches for kinetically mixed dark photons and for new particles as mediators connecting to the standard model (SM) constitute the prime dark-sector physics cases [1]. However, some dark states sharing a coupling to the SM photon have received comparatively less attention. In this scenario, even if dark states are perfectly electromagnetic (EM) neutral, higher-dimensional effective couplings to the SM photons are still possible. For dark states χ considered as a Dirac fermion, through various moments, such as magnetic dipole moments (MDM) and electric dipole moments (EDM) at mass-dimension five, and anapole moment (AM) and charge radius interaction (CR) at mass-dimension six, the couplings to the photon can be present [2,3].

In general, by interactions associated with photons, dark states χ with EM form factors can be produced, which therefore could be studied by accelerator-based experiments and stars. In Ref. [2], χ pair production in electron beams on fixed targets at NA64 [4], LDMX [5], BDX [6], and mQ [7] has been studied. In addition, constraints from rare meson (B and K) decays [8–10] and SM precision observables such as $(g-2)_\mu$ and the running of the fine-structure constant are also worked out. The current limits on and detection prospects of such dark-sector particles χ are illustrated in Ref. [11], utilizing high-intensity proton beams, concretely from LSND [12], MiniBooNE-DM [13], CHARM-II [14,15], and E613 [16] and projected SHiP [17] and DUNE [18,19]. Via their scattering of electrons in the Forward Liquid Argon Experiment detector at the LHC Forward Physics Facility, the prospects of searching for electromagnetically interacting χ particles have been studied in Ref. [20]. A detailed astrophysical study of stellar cooling constraints for the mass of dark states χ dropping below MeV is further complemented in Refs. [21,22]. Using missing energy searches at colliders, the constraints from e^+e^- colliders *BABAR* [2] and LEP [2,23], and from proton-proton collisions at LHC are also investigated [23,24].

In this paper, we extend the analysis to other electron colliders operated at the GeV scale, including BESIII [25], Belle II [26], and the proposed Super Tau Charm Factory (STCF) [27–29], which can probe the light dark states with a mass less than GeV scale. In order to accurately measure

*chenlw@impcas.ac.cn

the discovered Higgs, many high energy electron colliders are proposed, including the Circular Electron Positron Collider (CEPC) [30], Future Circular Collider e^+e^- (FCC-ee) [31], International Linear Collider (ILC) [32], and Compact Linear e^+e^- Collider (CLIC) [33]. We will take CEPC as an example to investigate the sensitivity on the dark state with EM form factor via higher-dimensional moments at future high energy electron colliders.

This paper is organized as follows. In Sec. II, we introduce the interactions between the dark states and photons. In Sec. III we describe the signal and backgrounds of probing the dark state with electromagnetic form factor at electron colliders. In Sec. IV we present the constraints on the corresponding couplings at BESIII, STCF, and Belle II that are operated with the c.m. energy $\sqrt{s} \ll M_Z$. In Sec. V, we consider the constraints at CEPC that are operated with $\sqrt{s} \geq M_Z$. Our conclusions are drawn in Sec. VI.

II. DARK STATES WITH ELECTROMAGNETIC FORM FACTOR INTERACTIONS

In this work, we consider that the dark state χ is taken as a Dirac fermion, which may have the effective interactions with the hypercharge gauge boson field B_μ as [2,24]

$$\mathcal{L}_\chi = \frac{1}{2}\mu_\chi^B \bar{\chi}\sigma^{\mu\nu}\chi B_{\mu\nu} + \frac{i}{2} d_\chi^B \bar{\chi}\sigma^{\mu\nu}\gamma^5\chi B_{\mu\nu} - a_\chi^B \bar{\chi}\gamma^\mu\gamma^5\chi\partial^\nu B_{\mu\nu} + b_\chi^B \bar{\chi}\gamma^\mu\chi\partial^\nu B_{\mu\nu}. \quad (1)$$

Here, $B_{\mu\nu} \equiv \partial_\mu B_\nu - \partial_\nu B_\mu$ is the hypercharge gauge field strength, μ_χ^B and d_χ^B are the dimensional coefficients of the mass-dimension-five MDM and EDM interactions, expressed in units of the Bohr magneton $\mu_B \equiv e/(2m_e)$ with e being the electric charge and m_e being the electron mass, and $\sigma_{\mu\nu} \equiv i[\gamma^\mu, \gamma^\nu]/2$; a_χ^B and b_χ^B are the dimensional coefficients of the mass-dimension-six AM and CR interactions. Hypercharge form factors are linear combinations of electromagnetic form factors and the corresponding Z boson operators, weighted by appropriate factors of the cosine and sine of the Weinberg angle c_W and s_W. Then Eq. (1) can be written with electromagnetic field strength tensor $F_{\mu\nu} \equiv \partial_\mu A_\nu - \partial_\nu A_\mu$ and Z gauge field strength tensor $Z_{\mu\nu} \equiv \partial_\mu Z_\nu - \partial_\nu Z_\mu$ as

$$\mathcal{L}_\chi = \frac{1}{2}\mu_\chi^\gamma \bar{\chi}\sigma^{\mu\nu}\chi F_{\mu\nu} + \frac{i}{2} d_\chi^\gamma \bar{\chi}\sigma^{\mu\nu}\gamma^5\chi F_{\mu\nu} - a_\chi^\gamma \bar{\chi}\gamma^\mu\gamma^5\chi\partial^\nu F_{\mu\nu} + b_\chi^\gamma \bar{\chi}\gamma^\mu\chi\partial^\nu F_{\mu\nu} + \frac{1}{2}\mu_\chi^Z \bar{\chi}\sigma^{\mu\nu}\chi Z_{\mu\nu} + \frac{i}{2} d_\chi^Z \bar{\chi}\sigma^{\mu\nu}\gamma^5\chi Z_{\mu\nu} - a_\chi^Z \bar{\chi}\gamma^\mu\gamma^5\chi\partial^\nu Z_{\mu\nu} + b_\chi^Z \bar{\chi}\gamma^\mu\chi\partial^\nu Z_{\mu\nu}, \quad (2)$$

with $\mathcal{C}_\chi^\gamma = \mathcal{C}_\chi^B c_W$ and $\mathcal{C}_\chi^Z = -\mathcal{C}_\chi^B s_W$ where $\mathcal{C}_\chi = \mu_\chi, d_\chi, a_\chi, b_\chi$.

In the scenarios of energies far below the electroweak scale, the Z boson degree of freedom decouples, and the effective interactions of Eq. (1) or (3) can be identically induced to

$$\mathcal{L}_\chi = \frac{1}{2}\mu_\chi \bar{\chi}\sigma^{\mu\nu}\chi F_{\mu\nu} + \frac{i}{2} d_\chi \bar{\chi}\sigma^{\mu\nu}\gamma^5\chi F_{\mu\nu} - a_\chi \bar{\chi}\gamma^\mu\gamma^5\chi\partial^\nu F_{\mu\nu} + b_\chi \bar{\chi}\gamma^\mu\chi\partial^\nu F_{\mu\nu}, \quad (3)$$

which has been investigated in Refs. [2,3,11,20–23]. The usual electromagnetic form factors should be denoted by the γ superscript, which will be omitted in the following for simplicity unless otherwise stated.

III. SIGNAL AND BACKGROUND AT e^+e^- COLLIDERS

The cross section for the single photon production from e^+e^- annihilation, $e^+e^- \to \chi\bar{\chi}\gamma$, can be approximately factorized into the process without photon emission, $e^+e^- \to \gamma/Z \to \chi\bar{\chi}$, times the improved Altarelli-Parisi radiator function [34,35],

$$\frac{d^2\sigma}{dx_\gamma dz_\gamma} = H(x_\gamma, z_\gamma; s)\sigma_0(s_\gamma), \quad (4)$$

where the radiator function is

$$H(x_\gamma, z_\gamma; s) = \frac{\alpha}{\pi}\frac{1}{x_\gamma}\left[\frac{1+(1-x_\gamma)^2}{1-z_\gamma^2} - \frac{x_\gamma^2}{2}\right]. \quad (5)$$

Here, s and s_γ are the square of the c.m. energies of the e^+e^- and $\chi\bar{\chi}$ system, respectively, with $s_\gamma = (1-x_\gamma)s$, E_γ being the energy of the initial state radiation (ISR) photon, $x_\gamma = 2E_\gamma/\sqrt{s}$ being the energy fraction emitted away by ISR, $z_\gamma = \cos\theta_\gamma$ with θ_γ being the polar angle of the photon. The cross section of the χ pair production without ISR σ_0 reads as

$$\sigma_0(s) = \frac{\alpha f(s)}{4 s^2}\sqrt{\frac{s-4m_\chi^2}{s}}\left[c_W^2 + (g_L+g_R)\frac{s(s-M_Z^2)}{(s-M_Z^2)^2+M_Z^2\Gamma_Z^2} + \frac{1}{2}\frac{1}{c_W^2}(g_L^2+g_R^2)\frac{s^2}{(s-M_Z^2)^2+M_Z^2\Gamma_Z^2}\right], \quad (6)$$

with $g_L = -\frac{1}{2} + s_W^2$, $g_R = s_W^2$, and M_Z and Γ_Z being the mass and decay width of the Z boson. The factor $f(s)$ is given as

$$\text{MDM: } f(s) = \frac{2}{3}(\mu_\chi^B)^2 s^2\left(1 + \frac{8m_\chi^2}{s}\right), \quad (7)$$

$$\text{EDM: } f(s) = \frac{2}{3}(d_\chi^B)^2 s^2\left(1 - \frac{4m_\chi^2}{s}\right), \quad (8)$$

$$\text{AM: } f(s) = \frac{4}{3}(a_\chi^B)^2 s^3 \left(1 - \frac{4m_\chi^2}{s}\right), \tag{9}$$

$$\text{CR: } f(s) = \frac{4}{3}(b_\chi^B)^2 s^3 \left(1 + \frac{2m_\chi^2}{s}\right). \tag{10}$$

In the following, we will present the results of the usual electromagnetic form factors $\mathcal{C}_\chi$ with $\mathcal{C}_\chi = \mathcal{C}_\chi^B c_W$.

It can be found that, in the limit of $\frac{m_\chi^2}{s} \to 0$, the production rates of the χ pair with the EM form factors for mass-dimension-five MDM and EDM operators have the same forms, as do mass-dimension-six AM and CR operators. When $\sqrt{s} \ll M_Z$, the production rate for a χ pair in Eq. (6) tends to be the same as the one that only considers dark sector-photon interactions [2].

For monophoton searches at electron colliders, the backgrounds consist of two categories: the irreducible background and the reducible background. The irreducible background arises from the neutrino pair production associated with one visible photon $e^+e^- \to \nu\bar{\nu}\gamma$. The reducible background comes from one visible photon in the final state together with several other SM particles that cannot be detected because of the detector limitations. The reducible background will be discussed later in detail for each experiment, since it strongly depends on the detector performance.

IV. e^+e^- COLLIDERS OPERATED WITH $\sqrt{s} \ll M_Z$

A. Belle II

The constraints on the light dark states with electromagnetic form factors from Belle II via monophoton searches have been investigated in Ref. [2], in which the authors follow Ref. [36], and scale up the *BABAR* background from Ref. [37] to an integrated luminosity of 50 ab^{-1} with the c.m. energy of 10.57 GeV, employ a constant efficiency cut of 50% in both search regions, and take identical geometric cuts for Belle II and *BABAR*. Reference [38] has provided the exact background subtraction in the monophoton search of Belle II to probe an invisibly decaying dark photon. In this work, we revisit the constraints from Belle II via monophoton searches following the strategy in Ref. [38].

At Belle II, the electromagnetic calorimeter (ECL), which covers a polar angle region of (12.4–155.1)° and has inefficient gaps between the barrel and the endcaps for polar angles between (31.4–32.2)° and (128.7–130.7)° in the lab frame [38]. The photons and electrons can be detected in the ECL. In the monophoton signature, the reducible background at Belle II consists of two major parts [39]: one is mainly due to the lack of polar angle coverage of the ECL near the beam direction, i.e., $\theta > 155.1°$ or $\theta < 12.4°$, which is referred to as the "bBG"; the other one is mainly owing to the gaps between the three segments in the ECL detector, i.e., $\theta \in (31.4\text{–}32.2)°$ or (128.7–130.7)°, which is referred to as the "gBG."

The bBG comes from the electromagnetic processes $e^+e^- \to \gamma + \not{X}$, dominated by $e^+e^- \to \gamma\gamma(\gamma)$ and $e^+e^- \to \gamma\ell^+\ell^-$. Here, $\not{X}$ denotes the other particle(s) in the final state that are emitted along the beam directions. Thus, except for the single detected photon, all the other final state particles are emitted along the beam directions with $\theta > 155.1°$ or $\theta < 12.4°$ in the lab frame, which are out of the cover polar angle region of the ECL.

At the asymmetric Belle II detector, for the monophoton events from reducible bBG, the maximum energy of the final photon in the c.m. frame E_γ^m is given by [39,40] (if not exceeding $\sqrt{s}/2$)

$$E_\gamma^m(\theta_\gamma) = \frac{\sqrt{s}(A\,\cos\theta_1 - \sin\theta_1)}{A(\cos\theta_1 - \cos\theta_\gamma) - (\sin\theta_\gamma + \sin\theta_1)}, \tag{11}$$

where all angles are given in the c.m. frame, and $A = (\sin\theta_1 - \sin\theta_2)/(\cos\theta_1 - \cos\theta_2)$, with θ_1 and θ_2 being the polar angles corresponding to the edges of the ECL detector. To remove the nasty bBG, the detector cut

$$E_\gamma^{\text{c.m.}} > E_\gamma^m \tag{12}$$

is adopted for the final monophoton (hereafter the "bBG cut"), with $E_\gamma^{\text{c.m.}}$ being the photon energy in the c.m. frame. Note that the "bBG" in the reducible background can be eliminated 100% by the "bBG cut" theoretically without considering other possible backgrounds that are caused by instruments.

In the gBG, the monophoton energy can be quite large around the $\theta_\gamma \sim 0$ region, because the gaps in the ECL are significantly away from the beam direction. The simulations for gBG have been carried out by Ref. [38] to search for an invisibly decaying dark photon. Two different sets of detector cuts are designed to optimize the detection efficiency for different masses of the dark photon: the "low-mass cut" and "high-mass cut." The "low-mass cut" can be described as $\theta_{\text{min}}^{\text{low}} < \theta_\gamma^{\text{lab}} < \theta_{\text{max}}^{\text{low}}$, where $\theta_{\text{min}}^{\text{low}}$ and $\theta_{\text{max}}^{\text{low}}$ are the minimum and maximum angles for the photon in the lab frame, respectively fitted as functions of [41]

$$\theta_{\text{min}}^{\text{low}} = 5.399°(E_\gamma^{\text{c.m.}})^2/\text{GeV}^2 - 58.82°E_\gamma^{\text{c.m.}}/\text{GeV} + 195.71°, \tag{13}$$

$$\theta_{\text{max}}^{\text{low}} = -7.982°(E_\gamma^{\text{c.m.}})^2/\text{GeV}^2 + 87.77°E_\gamma^{\text{c.m.}}/\text{GeV} - 120.6°. \tag{14}$$

The "high-mass cut" can be described as $\theta_{\text{min}}^{\text{high}} < \theta_\gamma^{\text{high}} < \theta_{\text{max}}^{\text{high}}$, where $\theta_{\text{min}}^{\text{high}}$ and $\theta_{\text{max}}^{\text{high}}$ can be respectively fitted as functions of [41]

$$\theta_{\min}^{\text{high}} = 3.3133°(E_\gamma^{\text{c.m.}})^2/\text{GeV}^2 - 33.58°E_\gamma^{\text{c.m.}}/\text{GeV} + 108.79°, \quad (15)$$

$$\theta_{\max}^{\text{high}} = -5.9133°(E_\gamma^{\text{c.m.}})^2/\text{GeV}^2 + 54.119°E_\gamma^{\text{c.m.}}/\text{GeV} - 13.781°. \quad (16)$$

In order to probe the sensitivity for the light dark states with electromagnetic form factors at Belle II, we use the definition

$$\chi^2(\mathcal{C}_\chi) \equiv \frac{S^2(\mathcal{C}_\chi)}{S(\mathcal{C}_\chi) + B + (\epsilon B)^2}, \quad (17)$$

where S (B) is the number of events in the signal (background) processes, ϵ is the background systematic uncertainty, and $\mathcal{C}_\chi = \mu_\chi, d_\chi, a_\chi, b_\chi$ denotes the dimensional coefficient of MDM, EDM, AM, and CR interactions, respectively. For background, $B = B_{\text{ir}} + B_{\text{re}}$ consists of the number of events in irreducible background B_{ir} and reducible background B_{re}. The number of events B_{ir} (S) can be obtained from the irreducible background (signal) by integrating the differential cross section in the phase space regions under the related detector cuts, and assuming photon detection efficiency as 95% [38]. It is found that about 300 (25000) gBG events survived the "low-mass cut" ("high-mass cut") with 20 fb^{-1} integrated luminosity [38] in the reducible background, which will be rescaled according to the considered luminosity. We show the numbers for an ideal case with zero systematics ($\epsilon = 0$) and also for a possible case with 10% systematics ($\epsilon = 10\%$).

By solving $\chi^2(\mathcal{C}_\chi) - \chi^2(0) = 2.71$, one can obtain the 95% confidence level (C.L.) upper limits on the corresponding electromagnetic form factors for dark states. The upper limits under "low-mass cut" and "high-mass cut" at Belle II with 50 ab^{-1} integrated luminosity are shown in Fig. 1. We can see that, assuming zero background systematics the

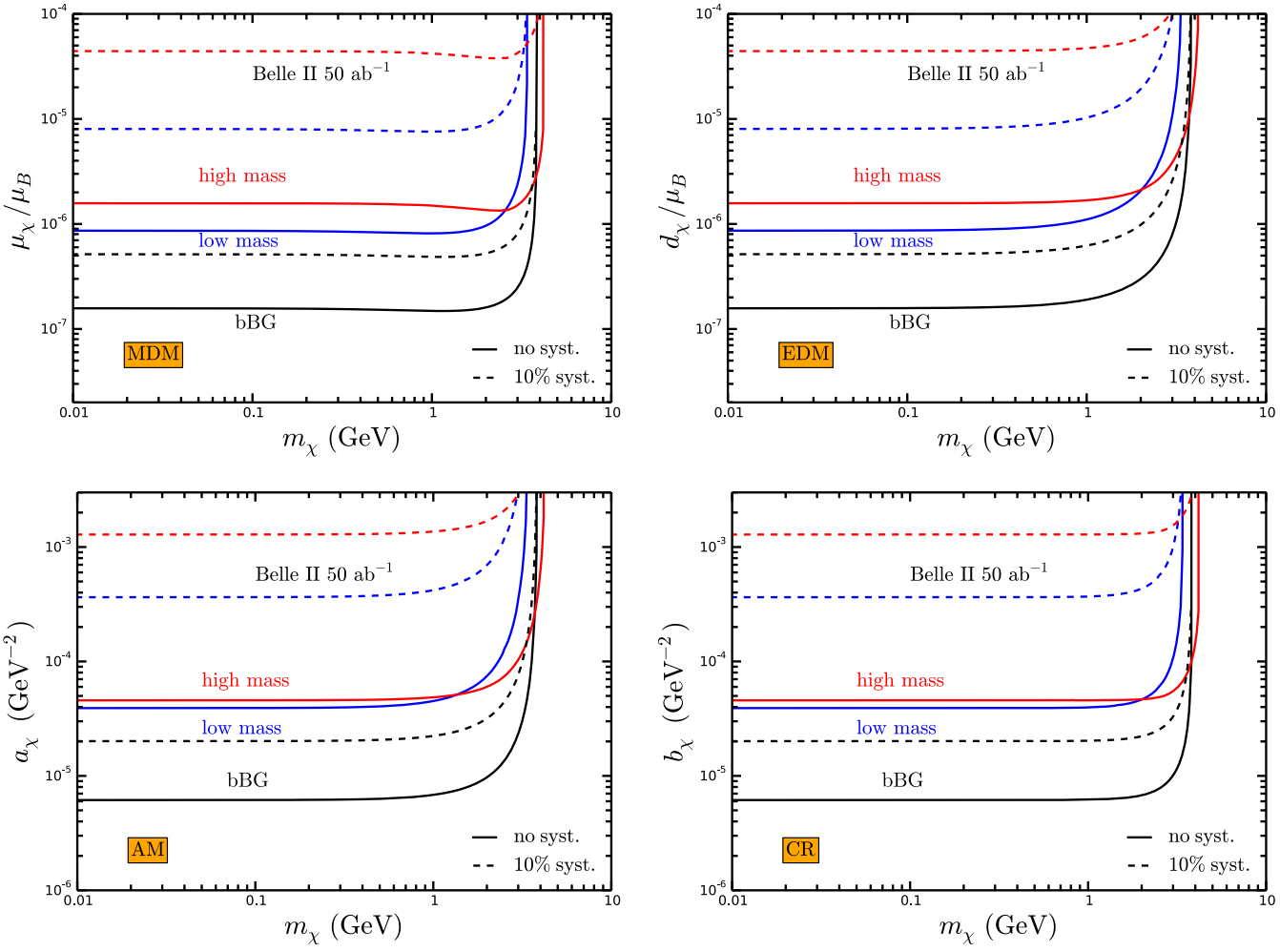

FIG. 1. The expected 95% C.L. upper limits on the electromagnetic form factors for mass-dimension-five operators through MDM (top left) and EDM (top right), and mass-dimension-six operators through AM (bottom left) and CR interaction (bottom right), at Belle II under "low-mass cut" (blue), "high-mass cut" (red), and "bBG cut" (black), with 50 ab^{-1} integrated luminosity. The solid (dashed) lines are assuming zero (10%) background systematics.

constraints under "low-mass cut" are better than "high-mass cut" for MDM with $m_\chi \lesssim 2.6$ GeV, EDM with $m_\chi \lesssim 2.1$ GeV, AM with $m_\chi \lesssim 1.4$ GeV, and CR with $m_\chi \lesssim 2.0$ GeV. The upper limits of the relevant interaction coefficients at 50 ab^{-1} Belle II can be down to about $8.6 \times 10^{-7}\mu_B$ ($8.0 \times 10^{-6}\mu_B$), and 3.9×10^{-5} GeV^{-2} (3.6×10^{-4} GeV^{-2}) for light dark state with mass-dimension-five and mass-dimension-six operators with zero (10%) background systematics, respectively. It is seen that for an ideal case with zero systematics, the sensitivity of Belle II on the electromagnetic form factors for dark states can improve by about 1 order relative to the case with 10% systematics. Thus the control on the systematic uncertainty on the background is very important.

In order to investigate the effects of the gBG, and compare with other experiments where detailed simulations with gBG being not available, the 95% C.L. upper limits without taking gBG into account are also presented in Fig. 1 labeled as bBG. In this scenario, the reducible background can vanish with the "bBG cut," and now the background events are all provided by the irreducible backgrounds that survived the "bBG cut." We find that the upper bound under the "bBG cut" can be down to about $1.6 \times 10^{-7}\mu_B$ (6.1×10^{-6} GeV^{-2}) for mass-dimension-five (six) operators, which is about five (six) times stronger than the one when gBG is considered under "low-mass cut." It should be noted that the Belle II bBG results cannot be interpreted as any actual sensitivity possible by the current Belle II experiment, while can explore the potential sensitivity of Belle II, if a new subdetector can detect the particles emitting from the gaps in ECL.

B. BESIII and STCF

The proposed STCF [27] in China is a symmetric double ring electron-positron collider. It is the next generation Tau Charm Facility and successor of the BESIII experiment, and designed to have c.m. energy ranging from 2 to 7 GeV. At BESIII and STCF, the cut for the final photon $E_\gamma > 25$ MeV in the barrel ($|z_\gamma| < 0.8$) or $E_\gamma > 50$ MeV in the end caps ($0.86 < |z_\gamma| < 0.92$) [42] is applied. Besides, we use the BESIII detector parameters to analyze the projected constraints from STCF due to the similarity of these two experiments. Since there is no released analysis of gBG at BESIII so far as we know, gBG in the monophoton reducible background at BESIII and STCF is not considered. Without taking gBG into account, the monophoton reducible background at BESIII and STCF mainly arises from $e^+e^- \to \gamma\gamma\gamma$ and $e^+e^- \to \ell^+\ell^-\gamma$. At symmetric BESIII and STCF, we also apply the detector cut [43,44]

$$E_\gamma > E_\gamma^m(\theta_\gamma) = \frac{\sqrt{s}}{(1+\sin\theta_\gamma/\sin\theta_b)} \tag{18}$$

on the final state photon to remove the reducible background, where θ_b denotes the angle at the boundary of the subdetectors. Taking into account the coverage of the main drift chamber, electromagnetic calorimeter, and time of flight, we have the polar angle $\cos\theta_b = 0.95$ at BESIII [45]. The photon detection efficiency is assumed as 100% at both BESIII and STCF in this work, since photon reconstruction efficiencies are all more than 99% [46] at BESIII.

Since 2012, the monophoton trigger has been implemented at BESIII, and the corresponding events have been collected with the luminosity of about 28 fb^{-1} at the c.m. energy ranging from 2.125 to 4.95 GeV until 2021. We compute the number of events due to signal (S) and backgrounds (B) under the applied cuts, and define $\chi^2_{\rm tot}(\mathcal{C}_\chi) = \sum_i \chi^2_i(\mathcal{C}_\chi)$, where $\chi^2_i(\mathcal{C}_\chi) \equiv S_i^2/(S_i + B_i + (\epsilon B_i)^2)$ with index i denoting each BESIII colliding energy. The expected 95% C.L. upper limits on the electromagnetic form factors of the light dark fermion χ according to about 28 fb^{-1} luminosity collected at BESIII are shown in Fig. 2 by demanding $\chi^2_{\rm tot}(\mathcal{C}_\chi) = \chi^2(0) + 2.71$. Figure 2 also shows the expected 95% C.L. upper limits with assumed 30 ab^{-1} luminosity at three typical colliding energies, $\sqrt{s} = 2, 4, 7$ GeV, in future STCF, respectively. The solid (dashed) lines are assuming zero (10%) background systematics. We find that BESIII can probe couplings down to about $1.1 \times 10^{-6}\mu_B$ for light dark states with mass-dimension-five operators and down to 1.0×10^{-4} GeV^{-2} with mass-dimension-six operators. The assuming 10% background systematics do not greatly affect the results at BESIII, since the backgrounds mainly from the irreducible background with gBG omitted are not significant. With the same luminosity, operated at lower energy, STCF has better sensitivity in probing the light dark fermion χ with the electromagnetic form factors though mass-dimension-five operators. This is because the monophoton cross section in small mass χ production is not very dependent on the c.m. energy, while in the background it decreases with the increment of the c.m. energy. On the contrary, for mass-dimension-six operators, the production rates of light dark states are even more sensitive to the center-of-mass energy; thus higher energy STCF has better sensitivity.

It should be noted that, as far as we know, BESIII has not released any analysis on the gBG. Thus for the BESIII and STCF analyses, the gBG is temporarily neglected in this work. Improved BESIII and STCF limits can be obtained in the future when the gBG analysis is available.

V. e^+e^- COLLIDERS OPERATED WITH $\sqrt{s} \geq M_Z$

A. LEP

The monophoton searches have been investigated carefully by all four LEP experiments [47]. In this work, we consider the limits on the cross section presented by the L3 Collaboration, both on the Z pole [48] with an integrated luminosity of 100 pb^{-1} at c.m. energies

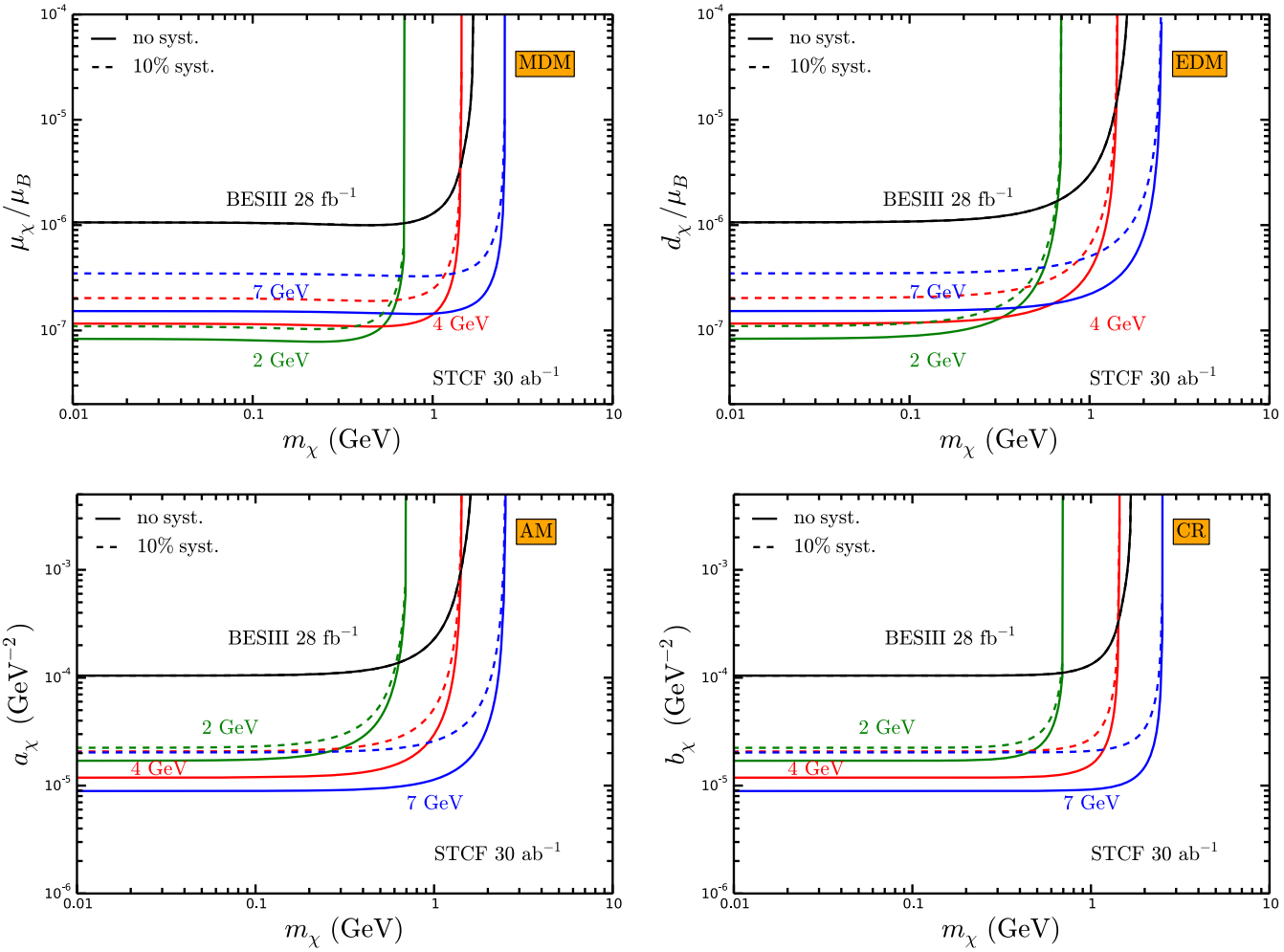

FIG. 2. The expected 95% C.L. upper limits on the electromagnetic form factors at BESIII and STCF, for mass-dimension-five operators (left) through MDM (top left) and EDM (top right), and mass-dimension-six operators through AM (bottom left) and CR interaction (bottom right). The limits from BESIII (black) are obtained with about 28 fb^{-1} integrated luminosity collected at the various c.m. energies ranging from 2.125 to 4.95 GeV during 2012–2021. The expected limits from STCF are shown at three typical energy points with 30 ab^{-1} integrated luminosity for $\sqrt{s} = 2$ (green), 4 (red), and 7 GeV (blue), respectively. The solid (dashed) lines are assuming zero (10%) background systematics.

$\sqrt{s} = 89.45$–91.34 GeV, and off the Z pole with 619 pb^{-1} at $\sqrt{s} = 188.6$–209.2 GeV [49]. Using the L3 off Z-pole data for the monophoton searches [49], the bounds in the presence of the χ couplings to only photons via mass-dimension-five MDM and EDM operators, and mass-dimension-six AM and CR operators have been studied in Refs. [2,23]. In this work, we revisit the sensitivity at LEP of the χ couplings to not only the photon but also the Z boson via Eq. (1) using the L3 measurements both on [48] and off [49] the Z pole. For comparison of cross sections at the Z pole, we require photon energy within the range 1 GeV $< E_\gamma <$ 10 GeV and the angular acceptance $45° < \theta_\gamma < 135°$, following the same event acceptance criteria as in Ref. [48] with six data subsets. Similarly, for the off Z-pole analysis, the high-energy photon should lie in the kinematic region $14° < \theta_\gamma < 166°$, and $p_T^\gamma > 0.02\sqrt{s}$, following the same event topology as described in Ref. [49] with eight data subsets. We obtain the bounds on the couplings from the data subset that leads to the best constraints using $|\sigma^{\rm SM} + \sigma^{\chi} - \sigma^{\rm exp}| \leq \delta\sigma^{\rm exp}$. Here $\sigma^{\rm SM}$ is the SM cross section, σ^{χ} represents the contribution from $\chi\bar{\chi}\gamma$ production, and $\sigma^{\rm exp} \pm \delta\sigma^{\rm exp}$ denotes the experiment result. We find that the off Z-pole measurement imposes a more stringent bound than the Z-pole measurement does, which can be seen in Fig. 4.

Owing to the couplings with the Z boson via Eq. (1), the dark sectors with $m_\chi < M_Z/2$ can now be constrained by invisible Z decay. The Z boson partial decay widths into $\chi\bar{\chi}$ mediated by hypercharge form factors can be expressed as

$$\Gamma_{Z\to\chi\bar{\chi}} = \frac{s_W^2 f(M_Z^2)}{16\pi M_Z}\sqrt{\frac{M_Z^2 - 4m_\chi^2}{M_Z^2}}. \tag{19}$$

The total width of the Z boson has been measured accurately by the LEP experiments which place a strong bound on beyond-the-SM contributions $\Gamma_{Z\to\chi\bar{\chi}} < 2.0$ MeV at 95% C.L. [50]. In Fig. 4, we show the constraints on the electromagnetic form factors for χ from the measurement of invisible Z decay at LEP. It can be found that the limits on dark states with electromagnetic form factors by invisible Z decay are stricter than those by monophton searches at LEP for MDM with $m_\chi \lesssim 45$ GeV, EDM with $m_\chi \lesssim 40$ GeV, AM with $m_\chi \lesssim 25$ GeV, and CR with $m_\chi \lesssim 40$ GeV.

B. CEPC

In the following, we will focus on the future CEPC [30,51]. The CEPC, proposed by the Chinese high energy physics community in 2012, is designed to run primarily at a center-of-mass energy of 240 GeV as a Higgs factory (H mode) with a total luminosity of 20 ab^{-1} for ten years running. In addition, it will also be operated on the Z pole as a Z factory (Z mode) with a total luminosity of 100 ab^{-1} for two years running at $\sqrt{s} = 91.2$ GeV, perform a precise WW threshold scan (WW mode) with a total luminosity of ~6 ab^{-1} for one year running at $\sqrt{s} \sim 160$ GeV, and be upgraded to a center-of-mass energy of 360 GeV, close to the $t\bar{t}$ threshold ($t\bar{t}$ mode) with a total luminosity of ~1 ab^{-1} for five years [52].

The monophoton signature, where the large missing transverse momentum carried away by the $\chi\bar{\chi}$ pair is balanced by a final state visible photon, is used to probe the dark states. Following the CEPC conceptual design report [30], the visible photon needs to satisfy the cuts $|z_\gamma| < 0.99$ and $E_\gamma > 0.1$ GeV. Beyond the irreducible background from the neutrino pair production in association with a visible photon $e^+e^- \to \nu\bar{\nu}\gamma$, any SM process with a single photon in the final state can contribute to the total background, with all other visible particles undetected. Since the SM processes which contain either jets or charged particles are relatively easy to distinguish from a dark state event, their contribution to the total background is negligible [53,54]. However, the exception is for the radiative Bhabha scattering, $e^+e^- \to e^+e^-\gamma$, which has a huge cross section and can mimic the signal if both the final state electrons and positrons escape undetected, for example, through the beam pipes. In our following analysis, we consider both neutrino and radiative Bhabha backgrounds.

To remove the monophoton events in the reducible background from the radiative Bhabha process $e^+e^- \to e^+e^-\gamma$, we apply the cut

$$E_\gamma > E_\gamma^m(\theta_\gamma) = \frac{\sqrt{s}}{(1+\sin\theta_\gamma/\sin\theta_b)} \tag{20}$$

on the final state photon following Ref. [43], where θ_b corresponds to the polar angle at the boundary of the subdetectors with $\cos\theta_b = 0.99$. For certain polar angle θ_γ, the maximum energy of the final photon E_γ^m in the reducible background occurs when the final state electron and positron emit along different beam directions with $\theta_{e^\pm} = \theta_b$.

Figure 3 shows the normalized energy distribution of final visible photon E_γ in the CEPC H mode ($\sqrt{s} = 240$ GeV) with detector cuts $E_\gamma > 0.1$ GeV and $|\cos\theta_\gamma| < 0.99$, for the irreducible background $e^+e^- \to \nu\bar{\nu}\gamma$ in SM and for dark state production through mass-dimension-five MDM and mass-dimension-six AM, respectively. It can be seen that the irreducible background exhibits a resonance peak in the monophoton energy spectrum which is centered at the photon energy $E_\gamma^Z = \frac{s-M_Z^2}{2\sqrt{s}}$ with a full-width-at-half-maximum as $\Gamma_\gamma^Z = M_Z\Gamma_Z/\sqrt{s}$ due to the SM Z boson. We will refer to this

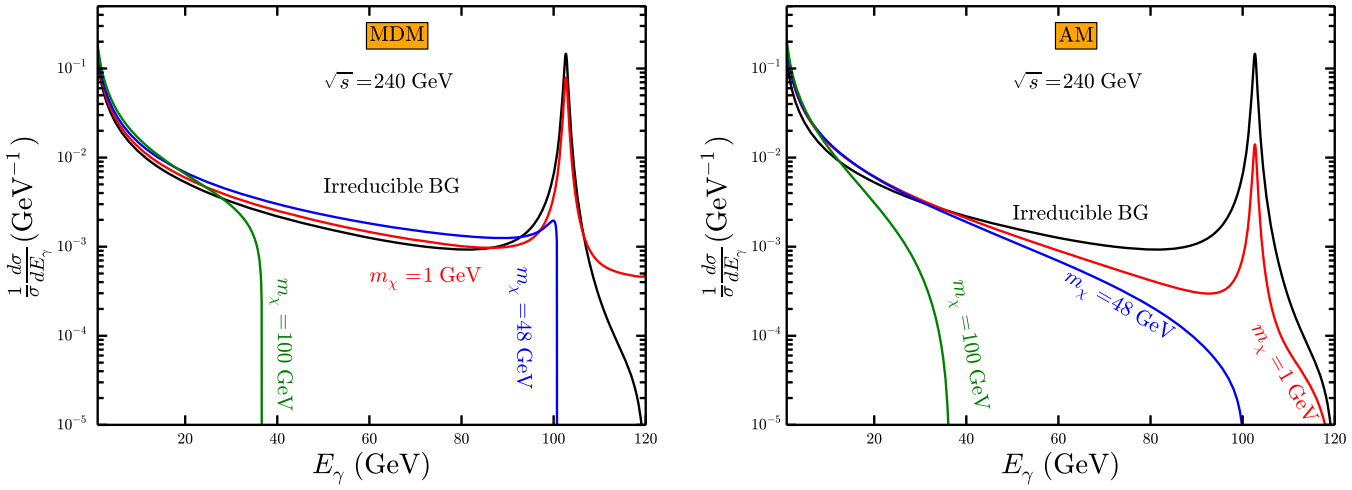

FIG. 3. Normalized E_γ distribution in the CEPC H mode ($\sqrt{s} = 240$ GeV) with detector cuts $E_\gamma > 0.1$ GeV and $|\cos\theta_\gamma| < 0.99$, for the irreducible background $e^+e^- \to \nu\bar{\nu}\gamma$ in SM and for dark state production through mass-dimension-five MDM (left) and mass-dimension-six AM (right). We consider three different masses in each case with $m_\chi = 1$ GeV, 48 GeV, and 100 GeV.

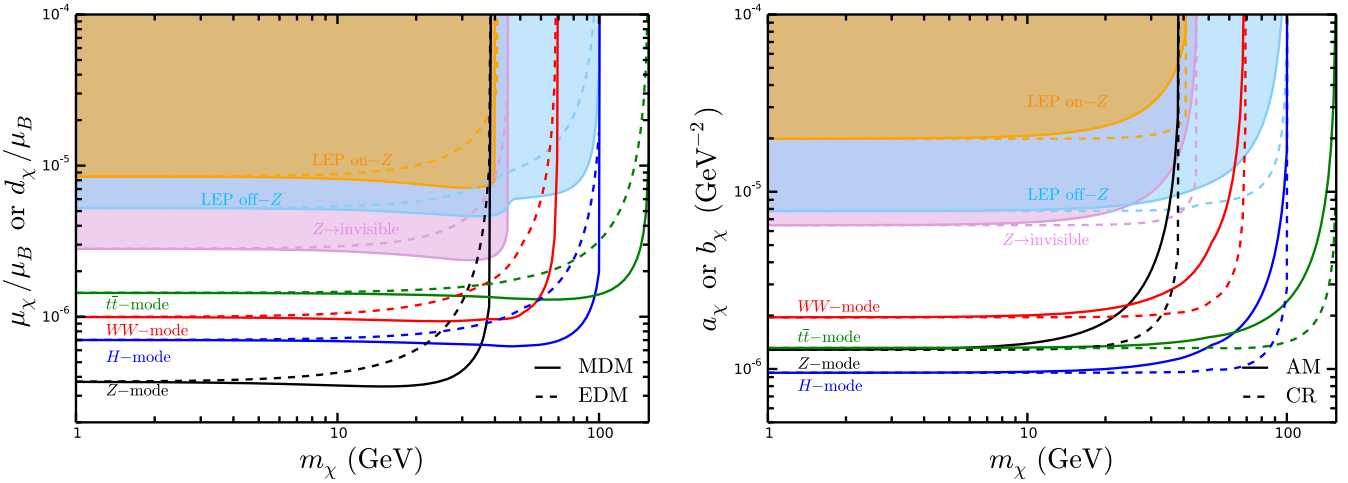

FIG. 4. The expected 95% C.L. upper limits on the electromagnetic form factors for mass-dimension-five operators (left) through MDM (solid) and EDM (dashed), and for mass-dimension-six operators (right) through AM (solid) and CR interaction (dashed) at CEPC in the Z mode with 100 ab^{-1} luminosity (black), in the H mode with 20 ab^{-1} luminosity (blue), and in the WW mode with 6 ab^{-1} luminosity (red), and in the $t\bar{t}$ mode with 1 ab^{-1} luminosity (green), respectively. The constraints at LEP from monophoton searches using the on [48] (orange) and off [49] (skyblue) Z-pole data and the measurement of invisible decay width of the Z boson [50] (purple) are also shown with shaded regions.

resonance in the monophoton energy spectrum as the "Z resonance" hereafter. To suppress the irreducible background contribution, we will veto the events within $5\Gamma_\gamma^Z$ at the "Z resonance" in the monophoton energy spectrum (hereafter the "Z resonance veto cut"). Though there is also a "Z resonance" in the light dark state production since the dark states can be produced via the their coupling with the Z boson, the "Z resonance veto cut" can also improve the ratio of signal to background. The final state photon associated with dark state production can have a maximum energy as m_χ, which is given by $E_\chi^m \equiv (s-4m_\chi^2)/(2\sqrt{s})$. Thus, to suppress the contributions from SM, we apply the following detector cuts at CEPC:

(1) $E_\gamma > 0.1$ GeV and $|\cos\theta_\gamma| < |\cos\theta_b| = 0.99$,
(2) $E_\gamma > E_\gamma^m(\theta_\gamma) = \sqrt{s}(1+\sin\theta_\gamma/\sin\theta_b)^{-1}$,
(3) $E_\gamma < E_\chi^m = (s-4m_\chi^2)/(2\sqrt{s})$,
(4) veto $E_\gamma \in 5\Gamma_\gamma^Z$.

We use the simple criteria $S^2/B = 2.71$ to study the 95% C.L. upper bounds on the couplings at CEPC, which are shown in Fig. 4. Here we compute the limits based on 20 ab^{-1} data in the H mode, 6 ab^{-1} data in the WW mode, 100 ab^{-1} data in the Z mode, and 1 ab^{-1} data in the $t\bar{t}$ mode. The Z mode has the best sensitivity for mass-dimension-five operators MDM with $m_\chi \lesssim 35$ GeV, and EDM with $m_\chi \lesssim 25$ GeV, which can probe the couplings down to about $3.7\times10^{-7}\mu_B$. The H mode has the best sensitivity for MDM with 35 GeV $\lesssim m_\chi \lesssim 98$ GeV, EDM with 25 GeV $\lesssim m_\chi \lesssim 79$ GeV, AM with $m_\chi \lesssim 63$ GeV, and CR with $m_\chi \lesssim 89$ GeV, and the corresponding couplings can be probed down to about $6.4\times10^{-7}\mu_B$, $1.1\times10^{-6}\mu_B$, 1.3×10^{-6} GeV^{-2}, and 9.8×10^{-7} GeV^{-2} respectively, for the case where $m_\chi \sim 50$ GeV by the H-mode running of CEPC. Although the luminosity of the $t\bar{t}$ mode is only one percent of that of the Z mode, the upper limits from the $t\bar{t}$ mode are still comparable to that of the Z mode for light dark states with mass-dimension-six operators, due to the fact that the production cross sections for χ are larger and the SM irreducible background is smaller in the $t\bar{t}$ mode than the Z mode. The $t\bar{t}$ mode has the best sensitivity for heavy dark states χ. With $m_\chi \sim 100$ GeV, $\mu_\chi \sim 1.4\times10^{-6}\mu_B$, $d_\chi \sim 3.2\times10^{-6}\mu_B$, $a_\chi \sim 2.4\times10^{-6}$ GeV^{-2}, and $b_\chi \sim 1.4\times10^{-6}$ GeV^{-2} can be probed by the $t\bar{t}$-mode running of CEPC.

VI. DISCUSSION AND CONCLUSIONS

The landscape of current excluded parameter space in the plane of dark state mass and coupling to the photon with mass-dimension-five (left panel) operators through MDM (solid) and EDM (dashed) and with mass-dimension-six (right panel) operators through AM (solid) and CR interaction (dashed) is shown in Fig. 5 by shaded regions, obtained from terrestrial experiments, such as proton-beam experiments CHARM-II or E613 [11], monophoton searches, Z-boson invisible decay at LEP and monojet searches at LHC [24], and astrophysics supernovae SN 1987A [21]. It should be noted that we only show several more competitive constraints in Fig. 5; the more complete results can be found in Refs. [2,11,20,21]. The 95% C.L. constraints on the dark states with electromagnetic form factors derived above from the electron colliders, BESIII, STCF, Belle-II, and CEPC, are also plotted with lines in Fig. 5. The Belle II limits (cyan lines) combine the low-mass and high-mass limits in Fig. 1, where both the bBG and the gBG are considered. To investigate the possible

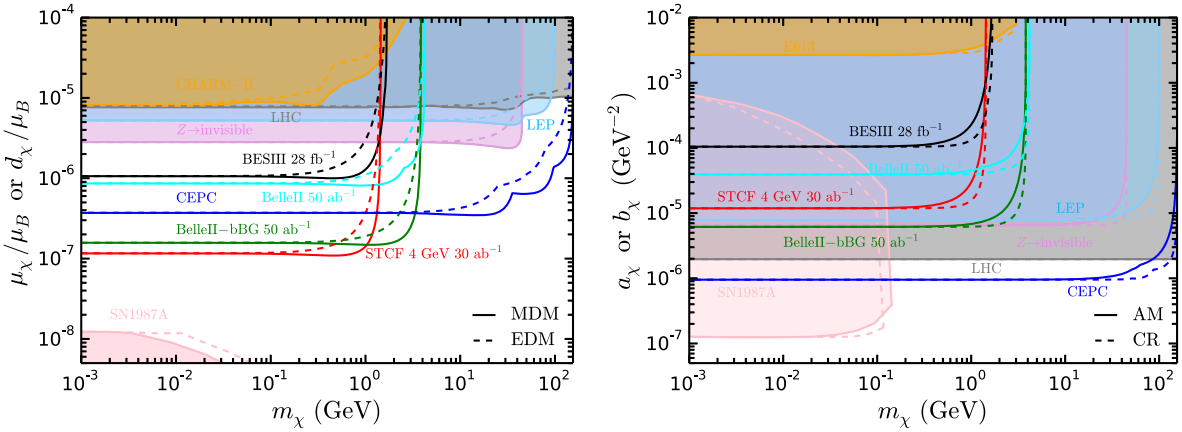

FIG. 5. The expected 95% C.L. exclusion limits on the electromagnetic form factors at electron colliders, including BESIII, STCF, Belle II, and CEPC, for mass-dimension-five operators (left) through MDM (solid) and EDM (dashed), and for mass-dimension-six operators (right) through AM (solid) and CR interaction (dashed). The Belle II limits (cyan lines) combine the low-mass and high-mass limits in Fig. 1, where both the bBG and the gBG are considered. The other Belle II limits (green lines) are obtained with the "bBG" cut where the gBG is omitted. The limits from BESIII (black lines) are obtained with about 28 fb^{-1} integrated luminosity collected at the various c.m. energies from 2.125 GeV to 4.95 GeV during 2012–2021. The STCF limits (red lines) are obtained with $\sqrt{s} = 4$ GeV and 30 ab^{-1}. The CEPC limits (blue lines) combine the best limits in Z mode, H mode, and $t\bar{t}$ mode in Fig. 4. The gBG is not considered at BESIII, STCF, and CEPC. The landscape of the current leading constraints are also shown with shaded regions, exploited from terrestrial experiments, such as proton-beam experiments CHARM-II or E613 [11], monophoton searches and Z-boson invisible decay at LEP, and monojet searches at LHC [24] and astrophysics supernovae SN 1987A [21].

potential of Belle II, and compare the sensitivity on the dark states-photon couplings with other electron colliders whose detailed simulations on gBG are not available, we also present the limits at Belle II (green curves) with gBG omitted. It is noted that the actual limits from BESIII, STCF, and CEPC should be weaker when gBG is taken into account.

For the mass-dimension-five operators, Z boson invisible decay is most sensitive with $m_\chi \lesssim 45$ (40) GeV through MDM (EDM) among the current constraints from the terrestrial experiments mentioned above. Monophoton search at the LEP is currently the strongest constraint in the range of 45 GeV $\lesssim m_\chi \lesssim$ 100 GeV through MDM. BESIII can probe new parameter space that is previously unconstrained by other experiments for mass $\lesssim$1 GeV, with 28 fb^{-1} data collected during 2012–2021. BESIII with the omission of the gBG (28 fb^{-1}) only leads to a slightly weaker limit than Belle II (50 ab^{-1}) with gBG included for $m_\chi \lesssim 1$ GeV. Although the STCF luminosity (30 ab^{-1}) is lower than Belle II (50 ab^{-1}), STCF has better sensitivity in probing the low-mass region ($m_\chi \lesssim 1$ GeV) than Belle II, if we assume that the gaps in the detector can be significantly suppressed in the future experiments, for instance, with a new subdetector that can detect the particles emitting from the gaps in ECL. This is because STCF is operated at a lower colliding energy ($\sqrt{s} = 4$ GeV) where the monophoton cross section in SM, mainly coming from irreducible neutrino backgrounds since the reducible QED backgrounds can be removed by the bBG cut, is smaller than Belle II ($\sqrt{s} = 10.58$ GeV), and $\chi\bar{\chi}\gamma$ production rate is not very dependent on the c.m. energy for mass-dimension-five operators. It is noted that the monophoton production rates from the reducible QED backgrounds, such as radiative Bhabha scattering $e^+e^- \to e^+e^-\gamma$, will grow with lower c.m. energies [44], thus potentially reducing the low-energy advantage of STCF over Belle II. The approximate 5 times the magnitude difference in sensitivity between the two Belle II limits, the cyan curve, and the green curve in Fig. 5 shows that the control on gBG is very important in probing the electromagnetic form factors via mass-dimension-five operators. When the background due to the gaps in the detectors is neglected, the future CEPC can give leading constraints than other electron colliders considered in this work when $m_\chi \gtrsim 4$ GeV, which can probe the coupling down to $3.7 \times 10^{-7}\mu_B$. While with about 100 ab^{-1} luminosity running at 91.2 GeV, the bounds on the light dark states from CEPC are still weaker than the ones from STCF and Belle-II with gBG omitted. It implies that the low-energy electron colliders can secure a place in the future to probe low-mass light dark states with electromagnetic form factors via mass-dimension-five operators, if the main reducible QED gBG can be significant suppressed, since there is significant uncertainty in understanding the reach of BESIII/STCF given that the main background rates are not known.

With regard to the mass-dimension-six operators, the bounds from the monojet search at LHC constrain better than other current experimental sensitivity in the plotted region in Fig. 5, except for the light dark states χ with

$m_\chi \lesssim 10$ MeV, which are constrained dominantly by the astrophysical bound from SN1987A. The upper limits from low-energy electron colliders, such as BESIII, STCF, and Belle II (except Belle II with gBG omitted), are all excluded by the monophoton search at LEP. This is because, for mass-dimension-six operators, the production rates of light dark states χ are even more sensitive to the c.m. energy, suggesting that it is unlikely for low-energy experiments to play any role in the foreseeable future. The high-energy colliders, such as CEPC, can probe a vast region of the parameter space that is previously unexplored, for the light dark states with electromagnetic form factors via mass-dimension-six operators through AM (CR) in the mass region from 20 MeV to 90 (140) GeV. Compared with current LHC bounds, the improvement on the upper limits of couplings is about 2 times the magnitude for the mass less than 10 GeV.

ACKNOWLEDGMENTS

This work was supported in part by the National Natural Science Foundation of China (Grants No. 12105327 and No. 11805001), the Natural Science Foundation of Anhui Province (No. 2208085MA10), and the Key Research Foundation of Education Ministry of Anhui Province of China (No. KJ2021A0061).

[1] R. Essig, J. A. Jaros, W. Wester, P. Hansson Adrian, S. Andreas, T. Averett, O. Baker, B. Batell, M. Battaglieri, J. Beacham *et al.*, arXiv:1311.0029.
[2] X. Chu, J. Pradler, and L. Semmelrock, Phys. Rev. D **99**, 015040 (2019).
[3] B. J. Kavanagh, P. Panci, and R. Ziegler, J. High Energy Phys. 04 (2019) 089.
[4] D. Banerjee *et al.* (NA64 Collaboration), Phys. Rev. D **97**, 072002 (2018).
[5] T. Åkesson *et al.* (LDMX Collaboration), arXiv:1808.05219.
[6] M. Battaglieri *et al.* (BDX Collaboration), arXiv:1607.01390.
[7] A. A. Prinz, R. Baggs, J. Ballam, S. Ecklund, C. Fertig, J. A. Jaros, K. Kase, A. Kulikov, W. G. J. Langeveld, R. Leonard *et al.*, Phys. Rev. Lett. **81**, 1175 (1998).
[8] C. Bird, P. Jackson, R. V. Kowalewski, and M. Pospelov, Phys. Rev. Lett. **93**, 201803 (2004).
[9] V. V. Anisimovsky *et al.* (E949 Collaboration), Phys. Rev. Lett. **93**, 031801 (2004).
[10] A. V. Artamonov *et al.* (BNL-E949 Collaboration), Phys. Rev. D **79**, 092004 (2009).
[11] X. Chu, J. L. Kuo, and J. Pradler, Phys. Rev. D **101**, 075035 (2020).
[12] C. Athanassopoulos *et al.* (LSND Collaboration), Nucl. Instrum. Methods Phys. Res., Sect. A **388**, 1492 (1997).
[13] A. A. Aguilar-Arevalo *et al.* (MiniBooNE DM Collaboration), Phys. Rev. D **98**, 112004 (2018).
[14] K. De Winter *et al.* (CHARM-II Collaboration), Nucl. Instrum. Methods Phys. Res., Sect. A **278**, 670 (1989).
[15] P. Vilain *et al.* (CHARM-II Collaboration), Phys. Lett. B **335**, 246 (1994).
[16] R. Ball, C. T. Coffin, H. R. Gustafson, L. W. Jones, M. J. Longo, T. J. Roberts, B. P. Roe, E. Wang, M. Duffy, G. Fanourakis *et al.*, eConf **C801002**, 172 (1980), https://www.slac.stanford.edu/econf/C801002/pdf/032.pdf.
[17] M. Anelli *et al.* (SHiP Collaboration), arXiv:1504.04956.
[18] R. Acciarri *et al.* (DUNE Collaboration), arXiv:1512.06148.
[19] B. Abi *et al.* (DUNE Collaboration), arXiv:1706.07081.
[20] F. Kling, J. L. Kuo, S. Trojanowski, and Y. D. Tsai, Nucl. Phys. **B987**, 116103 (2023).
[21] X. Chu, J. L. Kuo, J. Pradler, and L. Semmelrock, Phys. Rev. D **100**, 083002 (2019).
[22] J. H. Chang, R. Essig, and A. Reinert, J. High Energy Phys. 03 (2021) 141.
[23] J. F. Fortin and T. M. P. Tait, Phys. Rev. D **85**, 063506 (2012).
[24] C. Arina, A. Cheek, K. Mimasu, and L. Pagani, Eur. Phys. J. C **81**, 223 (2021).
[25] D. M. Asner, T. Barnes, J. M. Bian, I. I. Bigi, N. Brambilla, I. R. Boyko, V. Bytev, K. T. Chao, J. Charles, H. X. Chen *et al.*, Int. J. Mod. Phys. A **24**, S1 (2009), arXiv:0809.1869.
[26] T. Abe *et al.* (Belle-II Collaboration), arXiv:1011.0352.
[27] Q. Luo, W. Gao, J. Lan, W. Li, and D. Xu, *Proceedings of the IPAC2019* (JACoW Publishing, Geneva, Switzerland, 2019), 10.18429/JACoW-IPAC2019-MOPRB031.
[28] A. E. Bondar *et al.* (Charm-Tau Factory Collaboration), Phys. At. Nucl. **76**, 1072 (2013).
[29] X. D. Shi, X. R. Zhou, X. S. Qin, and H. P. Peng, J. Instrum. **16**, P03029 (2021).
[30] J. B. Guimarães da Costa *et al.* (CEPC Study Group), arXiv:1811.10545.
[31] A. Abada *et al.* (FCC Collaboration), Eur. Phys. J. Spec. Top. **228**, 261 (2019).
[32] H. Aihara *et al.* (ILC Collaboration), arXiv:1901.09829.
[33] A. Robson, P. N. Burrows, N. Catalan Lasheras, L. Linssen, M. Petric, D. Schulte, E. Sicking, S. Stapnes, and W. Wuensch, arXiv:1812.07987.
[34] O. Nicrosini and L. Trentadue, Phys. Lett. B **231**, 487 (1989).
[35] G. Montagna, O. Nicrosini, F. Piccinini, and L. Trentadue, Nucl. Phys. **B452**, 161 (1995).
[36] R. Essig, J. Mardon, M. Papucci, T. Volansky, and Y. M. Zhong, J. High Energy Phys. 11 (2013) 167.
[37] B. Aubert *et al.* (*BABAR* Collaboration), arXiv:0808.0017.
[38] E. Kou *et al.* (Belle-II Collaboration), Prog. Theor. Exp. Phys. **2019**, 123C01 (2019); **2020**, 029201(E) (2020).
[39] J. Liang, Z. Liu, Y. Ma, and Y. Zhang, Phys. Rev. D **102**, 015002 (2020).

[40] Y. Zhang, Z. Yu, Q. Yang, M. Song, G. Li, and R. Ding, Phys. Rev. D **103**, 015008 (2021).
[41] M. Duerr, T. Ferber, C. Hearty, F. Kahlhoefer, K. Schmidt-Hoberg, and P. Tunney, J. High Energy Phys. 02 (2020) 039.
[42] M. Ablikim *et al.* (BESIII Collaboration), Phys. Rev. D **96**, 112008 (2017).
[43] Z. Liu, Y. H. Xu, and Y. Zhang, J. High Energy Phys. 06 (2019) 009.
[44] Y. Zhang, W. T. Zhang, M. Song, X. A. Pan, Z. M. Niu, and G. Li, Phys. Rev. D **100**, 115016 (2019).
[45] Z. Liu and Y. Zhang, Phys. Rev. D **99**, 015004 (2019).
[46] M. Ablikim *et al.* (BESIII Collaboration), Phys. Rev. D **83**, 112005 (2011).
[47] R. L. Workman *et al.* (Particle Data Group), Prog. Theor. Exp. Phys. **2022**, 083C01 (2022).
[48] M. Acciarri *et al.* (L3 Collaboration), Phys. Lett. B **431**, 199 (1998).
[49] P. Achard *et al.* (L3 Collaboration), Phys. Lett. B **587**, 16 (2004).
[50] S. Schael *et al.* (ALEPH, DELPHI, L3, OPAL, SLD, LEP Electroweak Working Group, SLD Electroweak Group and SLD Heavy Flavour Group), Phys. Rep. **427**, 257 (2006).
[51] CEPC Study Group, arXiv:1809.00285.
[52] H. Cheng *et al.* (CEPC Physics Study Group), arXiv: 2205.08553.
[53] C. Bartels, M. Berggren, and J. List, Eur. Phys. J. C **72**, 2213 (2012).
[54] M. Habermehl, M. Berggren, and J. List, Phys. Rev. D **101**, 075053 (2020).